

## Kink instability of a highly deformable elastic cylinder

Apurba Lal Das<sup>1</sup> and Animesu Ghatak<sup>1</sup><sup>1</sup> Department of Chemical Engineering, Indian Institute of Technology, Kanpur 208016, India

PACS.68.35.Gy { First pacs description.

PACS.62.20.DC { Second pacs description.

PACS.62.20.-x { Third pacs description.

**Abstract.** { When a soft elastic cylinder is bent beyond a critical radius of curvature, a sharp fold in the form of a kink appears at its inner side while the outer side remains smooth. The critical radius increases linearly with the diameter of the cylinder while remaining independent of its elastic modulus, although, its maximum deflection at the location of the kink depends on both the diameter and the modulus of the cylinders. Experiments are done also with annular cylinders of varying wall thickness which exhibits both the kinking and the ovalization of the cross-section. The kinking phenomenon appears to occur by extreme localization of curvature at the inner side of a post-buckled cylinder.

Highly deformable, soft elastic materials occur in many different applications e.g. soft tissues, artificial organs, therapeutic patches, shock absorbers, dampeners, platforms for microfluidic devices etc. In these variety of applications the material is exposed to many different forms of mechanical loads, which, due to the large deformability of these materials, can generate such responses which are different from that commonly observed with the linear elastic systems. An example is the surface wrinkling which is the most common form of mechanical response in elastic objects subjected to compressive stresses e.g. engendered by bending of an elastic block [1], or by sliding of a rubber block over a hard surface [2] or by the transverse poisson contraction of a uniaxially stretched rubber sheet [3]; however, here we report a different kind of behavior observed with soft hydrogel under similar circumstances. Our experiments with hydrogel cylinders bent beyond a critical curvature show that instead of wrinkling, the material here responds by the appearance of one single sharp fold in the form of a kink at the inner side of the cylinder. As the cylinder is progressively bent, at a critical radius of curvature, the kink appears with an abrupt jump accompanied by the reversal of the curvature in the region close proximity to the kink; at the kink the curvature shoots up to infinity. While kinking phenomenon has been observed with slender biological elements like DNA [4] or bacterial flagella [5] and inorganic fibers like multi-walled nano-tubes [6], where kinks appear rather intrinsically, mediated by the dual effects of local defects and intermolecular interactions, the kinking phenomenon observed in our system appears to be akin to the classical Euler's buckling instability [7], albeit localized at the inner side of a post-buckled cylinder. In this letter we have characterized this instability by using solid and annular cylinders of varying inner and outer diameters and by varying the modulus of the gel material.

These gel samples were prepared by polymerization in water of Acrylamide as the monomer with the  $N,N'$ -Methylenebis-Acrylamide as the cross-linker (0.267% by weight of the monomer), TEMED as the promotor (0.004%) and Ammonium persulfate (0.04% by weight of the monomer) as the initiator. The monomer to water ratio was varied in such a way that the final product contained 60–95% by weight of water. The polymerization reaction was carried out in molds of different sizes to prepare samples of variety of thicknesses and diameters. The gel samples were washed in water for at least eight hours in order to remove any un-reacted monomer and cross-linker and were subjected to the experiment depicted in figure 1. Since, in the time scale of our experiment ( $\sim 1$  min) the gel samples behaved like an isotropic elastic solid, these were characterized by their shear modulus. The modulus was estimated by cantilever beam experiment [8] in which one end of the cylinder was clamped to a rigid support while the deflection of the free end under gravity was measured. Small enough length of the cylinder ensured that it did not stretch under gravity. We carried out also compression test [9] on the gel samples which yielded similar values for the modulus. Systematic variation of initial water content in the pre-polymer solution allowed us to produce gels of different modulus.

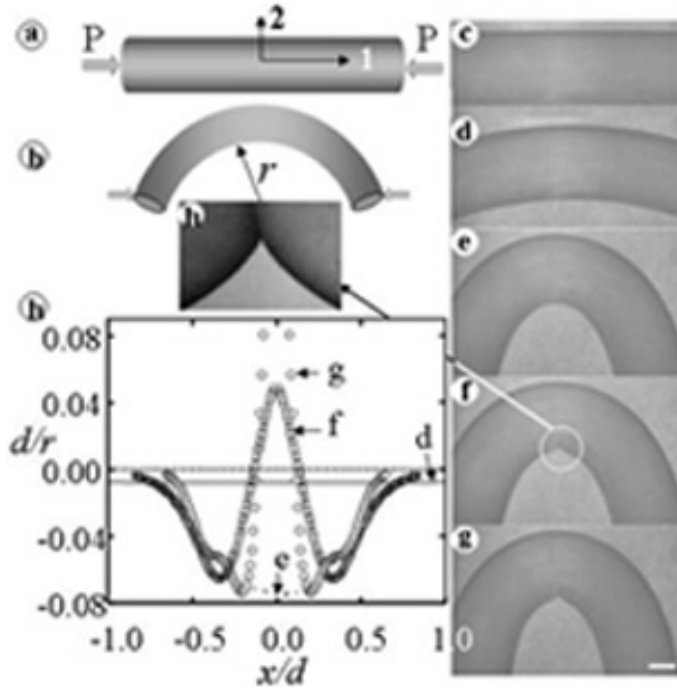


Fig. 1 (a) Schematic of the experiment, in which a straight gel cylinder of circular or rectangular cross-section is subjected to compressive end loads. (b) At a critical load, the cylinder buckles (Euler's buckling instability [7]), the curvature of which increases with further increase in the load. (c)–(g) A typical sequence of video-micrographs (captured using a video-camera having 25 fps resolution) leading to the appearance of the kink in a cylindrical gel cylinder of shear modulus 48 kPa and diameter  $d = 27$  mm. While (c) and (d) correspond to bending of the cylinder much before the appearance of the kink, micrograph (e) appears just before the occurrence of the kink in (f) and (g) corresponds to bending long after (f). Video-micrograph (h) depicts a magnified picture of the cylinder closed to the kink. (i) The curvature at the inner side of the cylinder in micrographs (d) to (g) are nondimensionalized as  $K = d/r$  and plotted with respect to its dimensionless length  $L = x/d$  along direction 1.

Figure 1 (a) and (b) depict the schematic of the experiment, in which cylinders of varying diameter (5–50 mm) and shear modulus (0.5–50 kPa) were subjected to compressive end loads between two rigid supports. Since very low modulus gels were observed to undergo deformation under their own weight, these gel samples were first immersed in water in which the samples remain neutrally buoyant and were then subjected to the experiment of Figure 1. In such experiments the straight cylinder did not remain stable but at a critical load underwent buckling; this phenomenon is the well-known Euler's buckling instability which resulted in smooth bending at both the inner and the outer sides of the rod; however, when the curvature at the inner side exceeded a critical value  $r_c$ , a sharp fold appeared in the form of a kink. Video-images 1 (c)–(f) represent a typical sequence as a cylinder of diameter  $d = 27$  mm and shear modulus  $\mu = 31$  kPa was progressively bent leading up to the appearance of the kink. While the Figure 1 (f) represents the frame at which the kink just appeared, frames (d) and (e) represent respectively a cylinder which was bent slightly and then critically; frame 1 (g) depicts the bending of the cylinder long after the appearance of the kink. The region closed to the kink is magnified in Figure 1 (h) which shows that curvature changed from negative to positive at the vicinity of the kink. This observation is quantified in Figure 1 (i) in which we plot the curvature of the inner side of the cylinder as it appears in images of Figure 1 (d)–(g) as a function of distance along the axis of the cylinder. The Figure shows that for images (c) and (d), the curvature is always negative through out the length of the cylinder; however in Figure 1 (e) the curvature changes abruptly to positive at the vicinity of the kink. In fact, at the kink, the curvature reaches infinity as the radius of curvature becomes zero. Thus curve (e) represents the critical bending after which curvature get localized within a distance  $\delta$  from the location of the kink. Once localized, the kink behaves like a hinge, so that, with further bending, the curvature does not change any significantly as evident from curve (g). Whereas all these experiments were done with temporal resolution of 0.04 sec, few experiments with higher resolution ( $\sim 0.001$  sec) showed [10] that the evolution of the kink was complete within a time scale of 0.001–0.005 second which was of the same order as that of the elastic deformation of the cylinder:  $\tau_b \sim (\mu/E)^{1/2} \sim 0.01$ – $0.001$  sec ( $\mu = 2$  mm,  $\rho = 1.0$  gm/cc,  $E = 50$  kPa). In fact this time scale was orders of magnitude smaller than the poro-elastic time scale proposed by Skotheim et al [11,12]:  $\tau_p = 10^2$ – $10^4$  sec [13]. Furthermore, in the reverse cycle, as the bending load was immediately withdrawn, the kink disappeared albeit at a slightly larger radius of curvature and the cylinder straightened out. However, in long time scale the kinking phenomenon was not completely reversible, because, when the cylinder was kept in the state as in frame 1f for a prolonged period (3–10 min), a defect appeared at the location of the kink, so that in subsequent cycles, the kink appeared at the same location at a much lower curvature. While this irreversibility is a signature of complex rheological character of the gel, we will concern here about its short time response only which is fairly reversible so that laws of elasticity are applicable.

We carried out experiments at fresh locations of the cylinders to obtain the data of critical radius of curvature  $r_c$ . The data for cylinders with varying diameter (3–50 mm) and modulus (5–50 kPa) as summarized in Figure 2 shows that all data fall on a single straight line with the result:  $r_c = 0.72d - 4.54$  implying the existence of a minimum diameter of the gel:  $d_{min} = 6.3$  mm, below which the kink did not appear. For these cylinders  $d < d_{min}$  mm, progressive bending resulted in increase in curvature while its inner and outer side remained smooth. For gel cylinders with  $d > d_{min}$ , the  $r_c$  remains independent of  $d$ . Interestingly, similar results were obtained also by Gent et al [1] in experiments with rubber block of shear modulus 1.5–1.8 MPa. Bending of rubber blocks of thickness  $h = 7$ – $14$  mm resulted in surface wrinkling at the inner side when the radius of curvature  $r_c = 0.72h$ . This similarity signifies that the critical curvature at which surface instabilities ensue remain unaltered over three

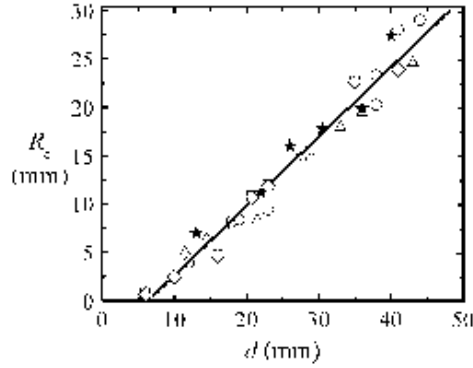


Fig. 2 { Critical inner radius of curvature at which the kink appears is plotted against the diameter of the cylinder. The symbols  $\circ$ ,  $\square$ ,  $\triangle$ ,  $\star$ ,  $\diamond$ , represent the data from experiments with gels of shear modulus 8, 14, 22, 31 and 45 kPa respectively. Data from experiments with cylinders of different modulus fall on a single straight line with result  $r_c = 0.72d - 4.54$ .

orders of magnitude in values of  $\mu$ , although, once ensued they evolve differently leading to either the wrinkles or the kink.

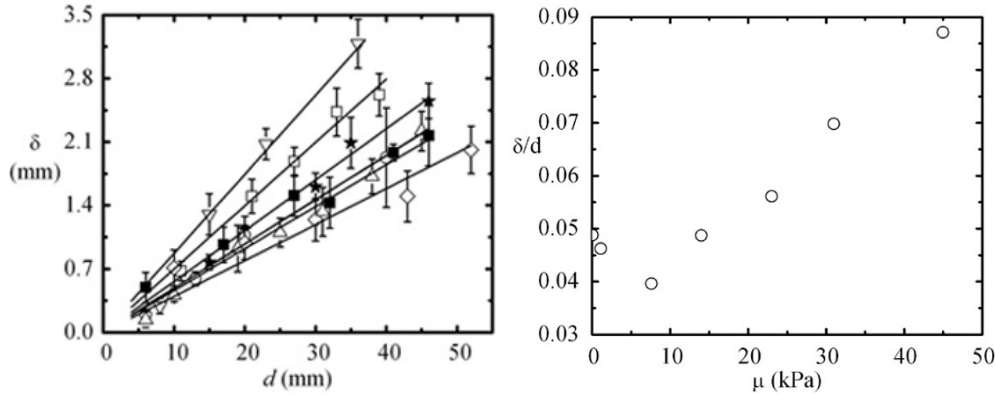


Fig. 3 { (a) The displacement of the gel at the location of appearance of the kink is plotted against the diameter  $d$  of the cylinder. The symbols  $\circ$ ,  $\square$ ,  $\triangle$ ,  $\star$ ,  $\diamond$ , represent gels of modulus 45, 31, 22, 14, 8, 1 and 0.5 respectively. (b) The slope  $\delta/d$  of these curves are plotted against the modulus of the gel.

The displacement at the kink however varies with both the diameter of the cylinders and their modulus.  $\delta$  increases linearly with the diameter but with  $\mu$ , it varies non-monotonically as shown in figure 3.  $\delta/d$  decreases in the range  $\mu = 0.5 - 1$  kPa but increases when  $\mu = 1 - 50$  kPa. This result shows that although geometry triggers the instability, its evolution is mediated by the dual effects of both the material and the geometric properties of the gel cylinders.

In order to further probe the effect of geometry we performed similar experiments with annular cylinders of which the thickness of the wall was varied. While for the solid cylinders, appearance of kink was the only mode of response, the annular ones responded by an additional mode: by ovalization of the cross-section of the cylinder, known as the Brazier effect [15]. The

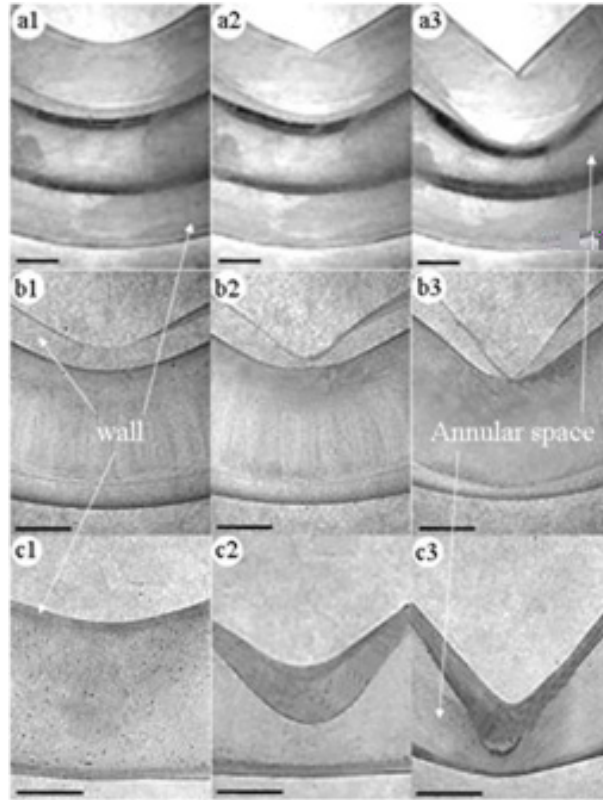


Fig. 4 { Annular gel cylinders are subjected to experiment in figure 1. Video-images  $a_i; b_i; c_i$  correspond to cylinders of inner diameter  $d_i = 26$  mm and wall thickness  $t_i = 28; 8$  mm and  $4$  mm respectively. In each series  $i = 1; 2$  and  $3$  correspond to images in successive frames respectively. In images  $a_i$  we see the appearance of the kink followed by the ovalization of the cross-section of the cylinder; in  $b_i$  both kink and ovalization occur simultaneously; whereas in  $c_i$  we see only the ovalization phenomenon.

images in figure 4 represent the typical patterns which were obtained when cylinders of inner diameter  $d_i = 26$  mm and wall thickness  $t_i = 4 - 28$  mm were subjected to bending. Here we see the appearance of not only the kinking instability as with solid cylinders, but also ovalization of its cross-section. Both these phenomena are captured in the sequence of images  $4a_1 - 3$  obtained while bending a cylinder of wall thickness  $t_i = 28$  mm. As bending exceeded the critical curvature, the kink appeared first at the inner side followed by the ovalization of its cross-section. These two phenomena however occurred simultaneously as the wall thickness decreased, as is evident in the sequence  $4b_1 - 3$  obtained with  $t_i = 8$  mm. Both the ovalization and the kinking instability are evident in figure  $4b_2 - b_3$ . When we further decreased the thickness to  $t_i = 4$  mm, we observed only the Brazier effect and not the kinking instability as in figure  $4c_1 - 3$ .

We rationalize our observations by considering the deflections of a rectangular elastic slab subjected to compressive stress [16]. A slab of thickness  $h_0$  and length  $L_0$  is compressed by an end stress  $P$  to length  $L = \alpha_1 L_0$  and thickness to  $h = \alpha_2 h_0$  where  $\alpha_1$  and  $\alpha_2$  are the initial compression ratios along  $x$  and  $y$  directions respectively;  $\alpha_3 = 1/\alpha_1 \alpha_2$  is that along  $z$ .

The slab buckles over and above this initial deformation following the stress equilibrium and incompressibility relations depicted in terms of the incremental stresses  $s_{11}$ ,  $s_{12}$  and  $s_{22}$  and displacements  $u$  and  $v$  along  $x$  and  $y$  respectively:

$$\begin{aligned} s_{11x} + s_{12y} - P w_y &= s_{12x} + s_{22y} - P w_x = 0 \\ u_x + v_y &= 0 \end{aligned} \quad (1)$$

The incremental quantities are related to the derivatives of displacements  $u$  and  $v$  as,

$$\begin{aligned} s_{11} &= s - 2u_x; s_{22} = s - 2v_y; s_{12} = -(u_y + v_x) \\ &= \frac{1}{2} \left( \frac{\partial u}{\partial x} + \frac{\partial v}{\partial y} \right)^2 \end{aligned} \quad (2)$$

where  $s$  is the average stress:  $s = (s_{11} + s_{22})/2$ . Equations 1 and 2 are solved using the boundary conditions that normal and shear traction on the free surfaces are zero:

$$f_x = s_{12} + P e_{xy} = 0 = f_y = s_{22} \quad (3)$$

The above equations have non-trivial solutions for the displacements, as long as the buckling load and the aspect ratio of cylinder satisfy the following conditions [16]:

$$\begin{aligned} 4k \tanh(k) - \frac{1 + k^2 \tanh^2(k)}{P} &= 0 \\ \text{where } k = \frac{\pi h}{L} \text{ and } P = \frac{P}{2} &= (1 + P/2) \end{aligned} \quad (4)$$

which in essence is a characteristic equation depicting the critical condition for buckling of the cylinder. While in the limit of a slender slab,  $L=h \gg 1$  i.e. when  $k \rightarrow 0$ , 4 yields the Euler's buckling load, in the other extreme of a thick semi-infinite slab i.e. when  $L=h \ll 1$  i.e.  $k \rightarrow \infty$ , it leads to a critical curvature at the inner side at which surface wrinkles appear. Gent et al [1] calculated this critical radius:  $r_c = h_0/0.36$  which is about half of that obtained in experiments. This discrepancy is explained if we consider that wrinkling is a local phenomenon and occurs over and above the buckling instability. In fact figure 1i suggests that the instability occurs within a distance  $L \sim h$ , so that  $k \sim 1$  and solving equation 4,  $k$  is obtained as 0.4. Following Gent et al's calculation [1], the critical radius of curvature is then obtained as  $r_c = h_0/0.6$  which is rather close to what was seen in experiments. Although this analysis captures the critical condition for occurrence of the instability, transient analysis of the system is needed in order to understand the evolution of the instability as well as displacement at the location of the kink.

To summarize, we have described here a new mode of surface undulation which results in a kink at the compressed side of a bent hydrogel cylinder. The timescale of evolution of this instability compares well with that of the elastic deformation of the material which implies that it is an elastic response of the material. The critical curvature at which the instability appeared could be captured by a simple approximate analysis but detail non-linear theory is needed to understand the evolution of the kink.

This work was supported by the Research initiation grant of IIT Kanpur.

Electronic address: aghatak@iitk.ac.in

## REFERENCES

- [1] A. N. Gent and I. S. Cho, *Rubber Chem. Technol.* 72, 253 (1999).
- [2] A. Schallamach, *Wear* 17, 301 (1971).
- [3] E. Cerda and L. Mahadevan, *Phys. Rev. Lett.* 90, 074302 (2003).
- [4] S. A. Koehler, T. R. Powers, *Phys. Rev. Lett.* 85, 4827 (2000).
- [5] J. W. Shaevitz, J. Y. Lee and D. A. Fletcher, *Cell* 122, 941 (2005).
- [6] A. E. Cohen and L. Mahadevan, *Proc. Natl. Acad. Sci.* 100, 12141 (2003).
- [7] A. E. H. Love, "A treatise on the mathematical theory of elasticity", Dover publications, New York 1944.
- [8] L. D. Landau and E. M. Lifshitz, "Theory of elasticity 3rd ed.", Butterworth-Heinemann, Oxford 2000.
- [9] E. C. Muniz and G. Geuskens, *Macromolecules*, 34, 4480 (2001).
- [10] A typical movie of the kinking instability can be seen in "<http://home.iitk.ac.in/~aghatak/Moviepage.htm>"
- [11] J. M. Skotheim and L. Mahadevan, *Proc. R. Soc. Lond. A*, 460, 1995 (2004).
- [12] Y. Forterre, J. M. Skotheim, J. Dumais and L. Mahadevan, *Nature* 433, 421 (2005).
- [13] Poroelastic timescale  $\tau_p = \frac{\eta}{kB}$  in which  $k$  is the hydraulic permeability of the gel,  $\eta$  is the viscosity of water inside the network and  $B$  is the bulk modulus of the dry gel. The quantity  $kB$  is a diffusion constant [14] which for our hydrogel samples should be  $10^{-8}$  to  $10^{-10} \text{ m}^2/\text{sec}$ . In our experiments,  $\eta = 1 \text{ cP}$  so that  $\tau_p = 100$  to  $10^4 \text{ sec}$ .
- [14] T. Tanaka, L. O. Hocker and G. B. Benedek, *J. Chem. Phys.* 59, 5151 (1973).
- [15] L. G. Brazier, *Proc. Roy. Soc. Lond. A* CXVI 104 (1926).
- [16] M. Biot, "Theory of incremental deformations", Dover publications, New York 1944.